TRICHOGIN TOPOLOGY AND ACTIVITY IN MODEL MEMBRANES AS DETERMINED BY FLUORESCENCE SPECTROSCOPY

B. Pispisa, L. Stella, C. Mazzuca and M. Venanzi [@]

2.1. INTRODUCTION

Antibiotic peptides, exhibiting activity against different types of microorganisms, are part of the innate immune system of most organisms.[1] Their mechanism of action is basically that of altering the permeability of cell membranes, bringing about the cell death by collapse of transmembrane electrochemical gradients and osmolysis,[2] though, despite the large number of studies, the molecular details of the mechanism are still uncertain.[3-5]

In view of the fact that bioactivity relies on both peptide affinity for membranes and ability to self-associate, it is easily understandable why cationic and hydrophobic peptides behave differently. Cationic peptides can bind to the charged surface of membranes, but their insertion in the hydrophobic core of the phospholipid bilayer or their aggregation is hindered by electrostatic effects. Therefore, their activity is best described by the Shai-Matsuzaki-Huang model, also known as the "carpet" or "toroidal pore" model, in which peptides bind to the membrane surface in a carpet-like fashion, by insertion into the polar headgroups region only. As a result, an unfavorable elastic tension arises, leading to the formation of transient defects or pores.[6] On the other hand, because hydrophobic peptides include in their sequence only a few or no charged amino acids, they tend to bring together, so that their mechanism of action is best described by the so-called "barrel stave" model, in which several peptide chains assemble in a transmembrane orientation, forming well defined channels. These two classes of peptides also differ in activity, in the sense that anionic lipids, such as those in bacteria, but not the zwitterionic bilayers, present in mammal or fungal cells, favor the binding of cationic peptides only.

[@] Department of Chemical Sciences and Technologies, University of Roma Tor Vergata, Rome, Italy I-00133

Therefore, these latter peptides are more selective than the hydrophobic ones. A similar difference holds in aqueous solution, in that the entropy-driven hydrophobic interactions definitely favor gathering, while the opposite occurs for cationic peptides, owing to electrostatic effects.

Lipopeptaibols[7] are members of a unique family of membrane active peptides, comprising a linear sequence of 6-10 aminoacids, a large amount of the helix-promoting Aib (α-aminoisobutyric acid),[8,9] a N-terminal fatty acyl group and a 1,2-amino alcohol at the C-terminus. One of the main components of this family is Trichogin GA IV (TR), a natural peptide having the following primary structure, where Oct is *n*-octanoyl, and Lol leucinol.

Oct-Aib^1-Gly^2-Leu^3-Aib^4-Gly^5-Gly^6-Leu^7-Aib^8-Gly^9-Ile^{10}-Lol (TR)

This peptide can modify membrane permeability, displaying both antibacterial and hemolytic effects. However, the full details of bioactivity are still unknown, and different models, including bilayer destabilization,[3] channel formation[10] or diffusion through the membrane as ion carrier,[11] have been put forward.

We report here the results of a thorough investigation on the behavior of this peptide in both aqueous solution and model membranes. Because peptide-membrane interactions are best studied by fluorescence experiments, two fluorescent trichogin analogs, both having a leucine methyl ester at the C-terminus, replacing Lol, were employed. One, denoted A3, is labeled with azulene [Aal: β-(1-azulenyl)-L-alanine], replacing Leu 3, and the other, labeled with a fluorene moiety (Fmoc: fluorenyl-9-methylcarbonyl group) linked to the side-chain of 2□-diamino-L-butyric acid (Dab), replacing Ile10, is denoted F10. The primary structure of the analogs is as follows, where TR-OMe is the reference peptide, and Boc a protective group (*t*-butyloxycarbonyl).

Oct-Aib-Gly-Leu-Aib-Gly-Gly-Leu-Aib-Gly-Ile-Leu-OMe (TR-OMe)
Oct-Aib-Gly-Aal-Aib-Gly-Gly-Leu-Aib-Gly-Dab(Boc)-Leu-OMe (A3)
Oct-Aib-Gly-Leu-Aib-Gly-Gly-Leu-Aib-Gly-Dab(Fmoc)-Leu-OMe (F10)

The fluorophores, chosen because they can act as a donor-acceptor pair in Förster energy transfer,[12] were incorporated in such positions as to substitute bulky side chains. This would minimize perturbations of peptide structure and activity.

2.2. PROPERTIES OF THE FLUORESCENT ANALOGS

To answer the question as to whether A3 and F10 peptides exhibit the same structural features and bioactivity of TR, both CD and peptide activity measurements, these latter based on peptide-induced leakage of small

unilamellar vesicles of ePC/cholesterol,* containing carboxyfluorescein, were carried out.

Figure 2.1 illustrates the far-UV CD spectra of TR-OMe, F10 and A3 in a structure-supporting solvent, such as methanol. The similarity of the spectra of Tr-OMe and F10 suggests that the Fmoc fluorescent label does not induce any significant structural perturbation, and that F10 analog exhibits the same structural features of TR. The CD spectrum of A3 is somewhat different, in the sense that the molar ellipticity is smaller than that of the other peptides. In all cases, the lowest accessible wavelength negative band falls at around 207 nm, and another negative band is observed at around 230 nm, the ratio of the molar ellipticity at the two wavelengths, $[\Theta]_{230}/[\Theta]_{207}$, being around 0.4 for TR-OMe and F10, and around 1 for A3. A value near 0.4 is suggestive of a right-handed 3_{10}-helical conformation.[13,14]

Interestingly enough, despite the fact that the fluorene moiety in F10 absorbs in this spectral region, an induced dichroic contribution was not detected, indicating that the fluorophore is not significantly perturbed by the asymmetric peptide chain. This, in turn, suggests that fluorene has a relatively high conformational mobility, in agreement with the fact that it is linked to the butyric side-chain. By contrast, azulene in A3 is less mobile than Fmoc in F10, because it is linked to the peptide backbone through a short side-chain, being thus capable of experiencing an induced dichroic contribution from the chiral

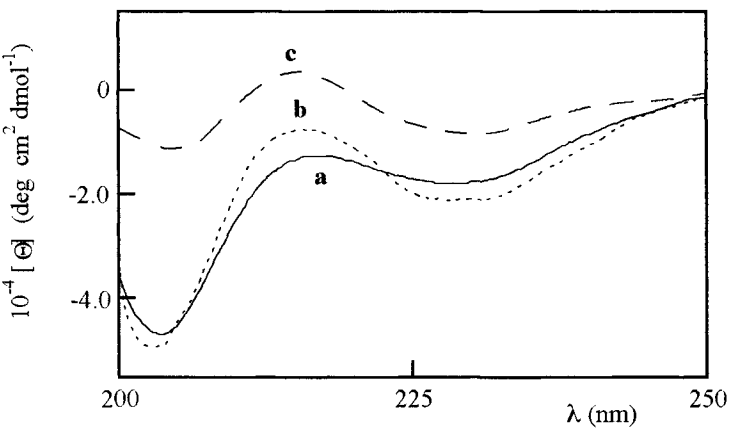

Figure 2.1. Circular dichroism spectra of TR-OMe (a), F10 (b) and A3 (c) in methanol.

* Liposomes were normally formed by egg phosphatidylcholine (ePC) and cholesterol (1:1 molar ratio). The experimental details are reported elsewhere. [17]

environment. This leads to a perturbation in the CD spectral patterns, as that observed, even if the structure is not altered.

As far as the CD spectra in water are concerned, they are reminiscent of unordered species, despite the presence of the helix-promoting Aib in the main chain. By contrast, when constrained in the bilayer, the peptides attain a α-helix conformation, as shown in Figure 2.2, where typical CD spectra in water and in membrane are reported. The conformational transition from a disordered state to α-helix on going from water to liposomes has been already observed for other peptide-membrane systems. It is often described as partition-folding coupling, which is thought to take place through a transient, prefolded state, into which the disordered peptide transforms, mediated by the membrane interface.[15,16] However, excluded volume effects are very likely sufficient to bring about the transition to an ordered structure.

The membrane permeability was estimated by measuring the peptide-induced release of a fluorescent marker (carboxyfluorescein), entrapped inside the liposomes. The results are shown in Figure 2.3, indicating that the behavior of A3, F10 and TR-OMe is quite similar.

To summarize, both F10 and A3 analogs exhibit structural characteristics and membrane permeability very similar to those of TR-OMe. Therefore, they can be considered as a good model of the natural trichogin peptide.

2.3. AGGREGATION IN WATER

Trichogin experiences aggregation in water because of its high hydrophobicity, which is also responsible for its insolubility, even at concentrations as low as 50 μM. Around the same concentration, aqueous solutions of TR-OMe, A3 or F10 are opalescent, suggesting that they aggregate,

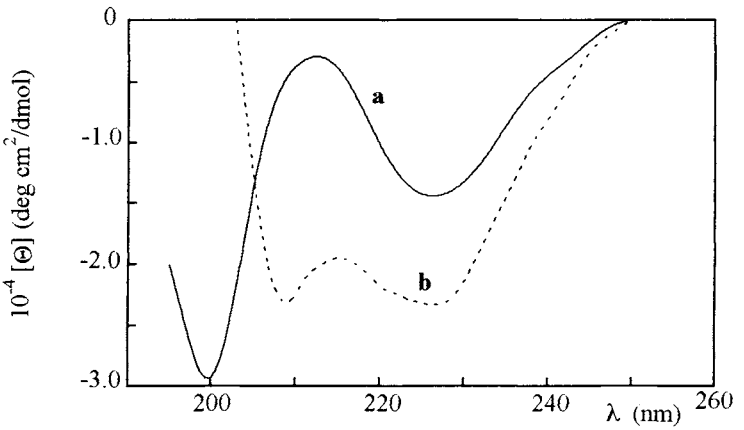

Figure 2.2. CD spectra of TR-OMe in water (a) and in membrane (b).

though ESR data show that this process is also accomplished in apolar solvents, such as toluene or chloroform,[11] thereby indicating that hydrophobicity is not the only driving force for aggregation to occur.

We then postulate the occurrence of the following two-state equilibrium:

$$n\,M \leftrightarrow M_n \tag{1}$$

where M is the monomer, M_n the aggregate, n the number of monomers in the aggregate and K the equilibrium constant, defined as:[17]

$$K^{n-1} = \frac{X'}{X^n} \tag{2}$$

X' and X being the molar fraction of aggregate and monomer, respectively. The total molar fraction of peptide, X_t, is then:

$$X_t = X + nX' \tag{3}$$

and the fraction of peptide chains partecipating to aggregates, f, is:

$$f = \frac{nX'}{X_t} \tag{4}$$

Fluorescence decay experiments prove that equilibrium (1) applies to the analogs examined in aqueous solution. For instance, Figure 2.4 illustrates the decay curve of F10 peptide at two concentrations, together with that of the reference, i.e. fluoren-9-acetic acid (Fmoc-OH). The decay curve of Fmoc-OH is well described by a single exponential ($\tau = 5.6 \pm 0.1$ ns; $\chi^2 = 1.0$), while that

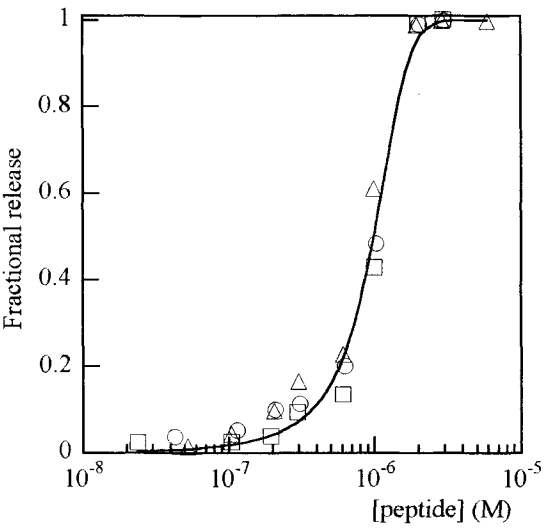

Figure 2.3. Perturbation of the bilayer by TR-OMe (circles), F10 (triangles) and A3 (squares): peptide-induced release of carboxyfluorescein from the bilayer. [Lipid] = 60 μM. The fractional release was determined 20 min after peptide addition.

of F10 by a biexponential function, having lifetimes $\tau_1 = 5.6 \pm 0.1$ ns and $\tau_2 = 0.87 \pm 0.08$ ns ($\chi^2 = 1.0$), irrespective of concentration. In principle, each decay time could arise either from a single species or from many species, all having a similar quenching rate. This latter hypothesis implies that all these species have very similar structural and geometric features, so that they are indistinguishable within the resolution time.

Where the pre-exponential factors of the shortest lifetime component is reported as a function of peptide concentration, the plot of Figure 2.5 is obtained. The data are well fitted by the following expression, derived from Eqs. (2)-(4):[17]

$$f = n(1-f)^n(KX_t)^{n-1} \tag{5}$$

This finding validates the occurrence of a two-state equilibrium, such as that of Eq. (1). Therefore, the longest lifetime component may be reasonably assigned to the monomeric species M, while the shortest one is assigned to the oligomeric species M_n. From the fitting, one obtaines $n = 2.3 \pm 0.3$ and $K = (3.4 \pm 0.2)\ 10^7$, n being a Hill-like parameter, because, according to Eq. (1), the aggregation equilibrium is cooperative, i.e., to a first approximation, intermediate aggregates other than the species M_n are minor. A narrow distribution of aggregates is likely to reflect assemblies with similar size and geometry, fully compatible with a single lifetime. The parameter n thus represents the lowest limit of the number of peptide chains partecipating to the gathering process.

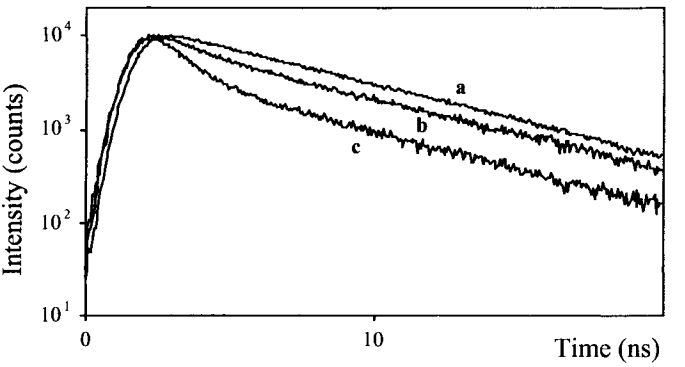

Figure 2.4. Fluorescence decay curves of the reference (Fmoc-OH; a) and of F10, at two concentrations: 1.9 μM (b) and 11 μM (c) in aqueous solution. The best fit of the reference is accomplished by a monoexponential function, while that of the peptide by a biexponential function. $\lambda_{ex} = 265$, $\lambda_{em} = 315$ nm.

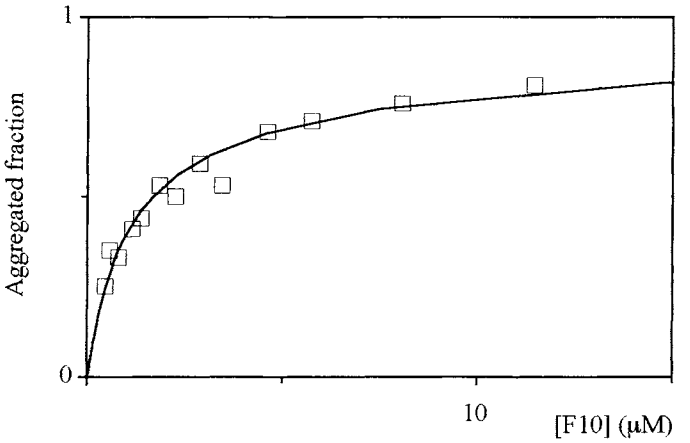

Figure 2.5. Pre-exponential factors of the short lifetime component of F10 decay in water, corresponding to the molar fraction of aggregated peptide (squares), as a function of [F10]. The solid line represents the best fit to the experimental data, according to Eq. (5).

2.4. WATER-MEMBRANE PARTITION AND AGGREGATION

Preliminarly, we measured the change in fluorescence intensity caused by the addition of different amounts of liposome into peptide aqueous solutions. The results are reported in Figure 2.6, where the partiton curves show that, as peptide concentration increases, association with the phospholipid bilayer is progressively less favored, a finding suggestive of a complex partition equilibrium, very likely involving aggregated species, too.[17,18]

To answer the question as to whether the peptides are actually inserted into the membrane, and, in such a case, which species predominate, both collisional quenching and time-resolved fluorescence experiments were carried out. As far as the collisional measurements are concerned, the efficiency of water soluble quenchers was determined to assess the accessibility of membrane-bound fluorophores from the water phase.[19] Figure 2.7 illustrates the Stern-Volmer plots corresponding to the iodide quenching of 1.0 μM F10 and A3. The results clearly show that for both analogs the quenching caused by iodide ions is significantly reduced by the presence of liposomes, indicating that the peptides are inserted into the membrane. However, the probes still exhibit a partial accessibility to the quencher, azulene appearing somewhat more accessible than fluorene, probably because of its polarity, bringing it close to the polar headgroups for electrostatic effects.

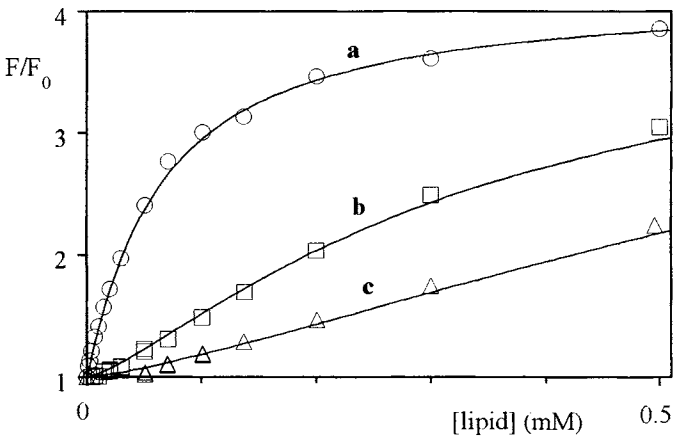

Figure 2.6. Water-membrane partition of F10, as measured by the fluorescence intensity of the peptide (F), normalized by that in the absence of membrane (F_0). [F10] = 1.1 μM (a), 11 μM (b) and 30 μM (c).

Time-resolved fluorescence measurements, within the $5 \cdot 10^{-3}$ - $65 \cdot 10^{-3}$ range of the total peptide/lipid molar ratio explored (at two phospholipid concentrations: 0.2 and 2.0 mM), were performed under the condition that the membrane-bound peptide is in equilibrium with the free peptide in water. As expected, the fluorescence decay was complex, because of the contribution of the species in the bilayer, besides those present in water. A typical decay curve is shown in Figure 2.8, referring to F10. After different trials, a good fit to the experimental data was obtained by a four exponential function, assuming that two species are present in the membrane phase, too. Besides the two lifetime components observed in pure water (Figure 2.5), that were taken fixed at 5.6 and 0.87 ns, the other two components were left free for the global fit of the fluorescence decay. As a result, one obtains $\chi^2 = 0.95$ and a satisfactory residuals distribution.

The two decay components associated to the membrane-bound species were $\tau'_1 = 7.0 \pm 0.2$ ns and $\tau'_2 = 2.2 \pm 0.2$ ns, both being significantly longer than in water, as expected for the increase in fluorescence intensity caused by membrane binding. The relative population of each component is reported in Figure 2.9. From the results, it appears that the weight of the longest lifetime in the membrane decreases as peptide concentration increases, as one would predict for a membrane-bound monomer; consequently, the other component (τ'_2) is assigned to the oligomer. This hypothesis is supported by the finding that the aggregate is almost completely quenched as compared to the monomer, as already observed in water. A multi-exponential decay could be also due to other effects, such as a slow relaxation of membrane system, a different environment around the fluorophore, different states of the peptide,[20] and,

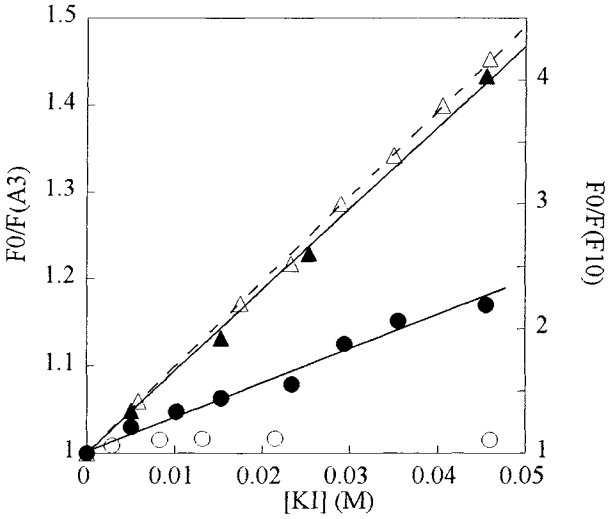

Figure 2.7. Stern-Volmer plots of collisional quenching by iodide ions for A3 (full symbols) and F10 (empty symbols). [A3] and [F10] = 1 μM in water (triangles) and in the presence of liposomes (circles).

finally, a concentration-induced change in orientation of the peptide inside the bilayer.[21] The observation that the fluorescence decay of membrane-bound peptide depends on peptide concentration rules out both conformational heterogeneity of the peptide and solvent/membrane relaxation phenomena. Therefore, besides the monomer-aggregate equilibrium, a concentration-induced change in orientation may contribute to the observed multi-exponential decay.

The following scheme summarizes the overall results.

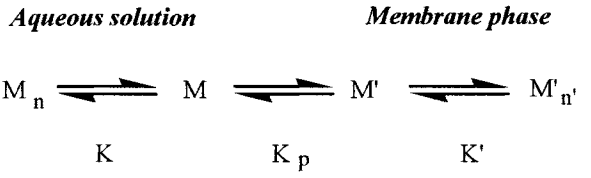

In this scheme, the equilibrium $M_n \leftrightarrow M'_{n'}$ is not taken into account, because the aggregate in the two phases exhibit a different size and, possibly, structure (see below), ascribable to the different environment. Therefore, M_n and $M'_{n'}$ species can not be related by a simple partition equilibrium. Furthermore, the prime refers to the species in the membrane, K and K' to the equilibrium

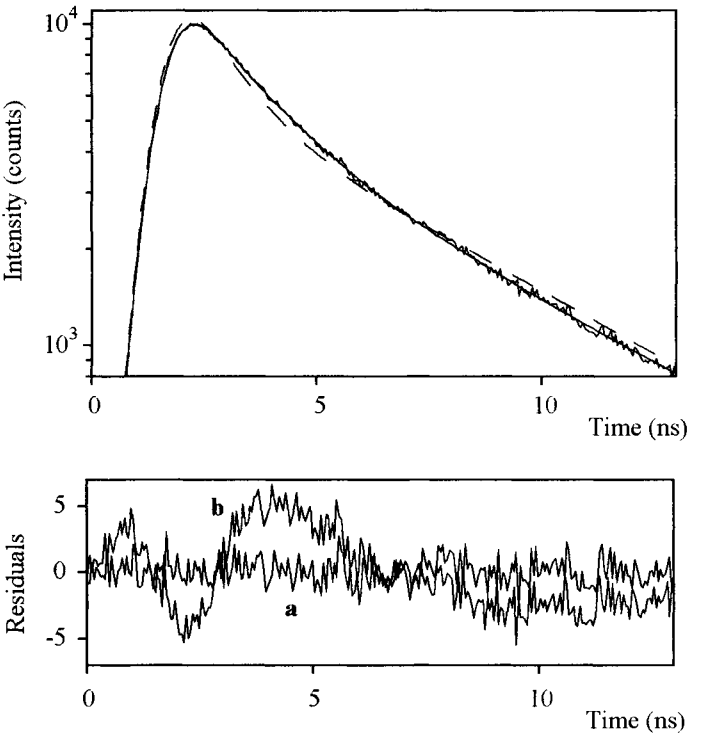

Figure 2.8. Fluorescence decay curves of F10 (50 μM) in the presence of 2 mM ePC/cholesterol (1:1); λ_{ex} = 265, λ_{em} = 315 nm. The dashed line represents the fit to the experimental data by a triple exponential function, with two lifetimes fixed at 5.6 and 0.87 ns, as those observed in pure water, and the third one left free (χ^2 = 4.6). By contrast, the solid line represents the fit to the data by a four exponential function, in which two lifetimes were still maintained fixed, and the other two were left free for the global fit of the fluorescence decay (χ^2 = 0.95). The residuals clearly show how the four exponential function (a) is definitely better than the triple one (b).

constant of aggregation in water and membrane, respectively, and K_p to the equilibrium constant of the water-membrane partition, linked to the change in the overall standard free energy of transfer by the following expression:[22,23]

$$\Delta G^0_{tr} = -RT\ln K_p = \Delta G^0_{solv} + \Delta G^0_{bilayer} \quad (6)$$

In Eq (6), ΔG^0_{solv} is the change in the standard free energy of solvation of the peptide and membrane upon partitioning, and $\Delta G^0_{bilayer}$ that arising from both perturbation of the peptide conformation caused by the bilayer, and perturbation of the lipid structure upon partitioning and binding processes.[16,22-24] No coulombic term is present because the peptides examined have no

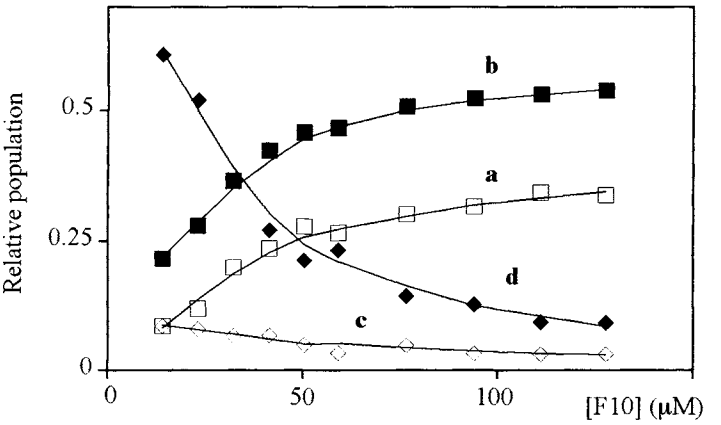

Figure 2.9. Pre-exponential factors from fluorescence decay curves of F10 in 2 mM ePC/cholesterol (1:1), corresponding to the following lifetimes: 0.87 ns (a), 2.2 ns (b), 5.6 ns (c) and 7.0 ns (d); see text.

charged residues. Owing to the composite nature of both free energy changes, it is quite difficult to estimate ΔG^0_{solv} and $\Delta G^0_{bilayer}$. The sole quantity that can be confidently evaluated is the total standard free energy change of transfer, i.e. $\Delta G^0_{tr} = -1.8$ kcal $\cdot mol^{-1}$, as obtained from the value of K_p reported below.

Interestingly, the value of ΔG^0_{tr} is much smaller than that of, say, the transfer of hydrocarbons from water to an organic solvent. For instance, for n-$C_{10}H_{12}$ at 25°C, $\Delta G^0_{tr} \approx -11$ kcal$\cdot mol^{-1}$.[25] In our case, however, there are contributors of opposite sign that partially balance, giving rise to a relatively small value of ΔG^0_{tr}. For example, contributors with positive sign are the variation in conformational free energy and, possibly, in desolvation free energy of the peptide upon transferring from water to the membrane.

We next examined each equilibrium reported in the foregoing scheme, separately.[17] The results are shown in Figures 2.10 and 2.11. The main inference to be drawn from these Figures is 3-fold. Firstly, the water-membrane partition equilibrium is characterized by a constant value of the fraction of the monomer associated to the membrane, within the $5 \cdot 10^{-3}$ - $65 \cdot 10^{-3}$ range of the total peptide/lipid molar ratio explored (data not shown). This implies the occurrence of a true equilibrium, whose constant is $K_p = (1.3 \pm 0.3)10^3$. Secondly, the results referring to aggregation in water are similar to those obtained in pure water and already reported in Figure 2.5, all data being satisfactorily fitted by a single curve, as illustrated in Figure 2.10. Thirdly, the curve describing the aggregation equilibrium in membrane (Figure 2.11) shows

that this process is much less favored and much more cooperative than that in water. The best fit of these latter data by eq (5) gives n' = 8.0 ± 3 and K' = 154 ± 8, implying that the average size of the aggregate in membrane is definitely larger than in water. This very likely reflects the peptide state of being ordered and constrained.

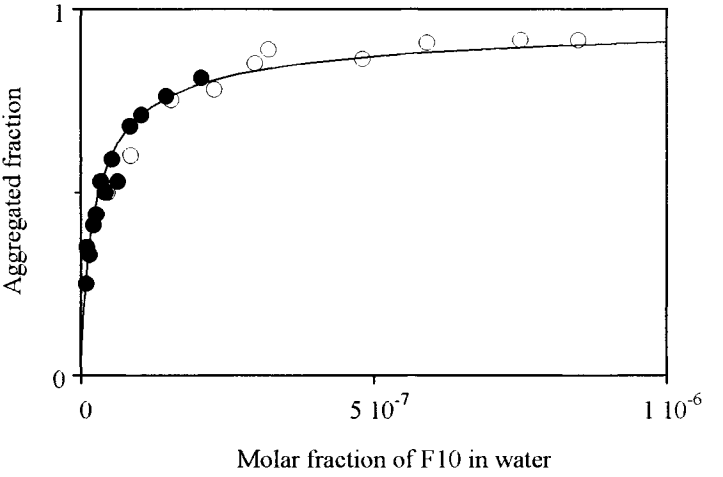

Figure 2.10. Aggregation data of F10 in water (empty circles), as obtained by the time-resolved curves in the presence of liposomes (Figure 2.9). The results referring to the aggregation in pure water are also reported as full circles, for comparison. The solid line is the best fit to the overall data, according to Eq. (5).

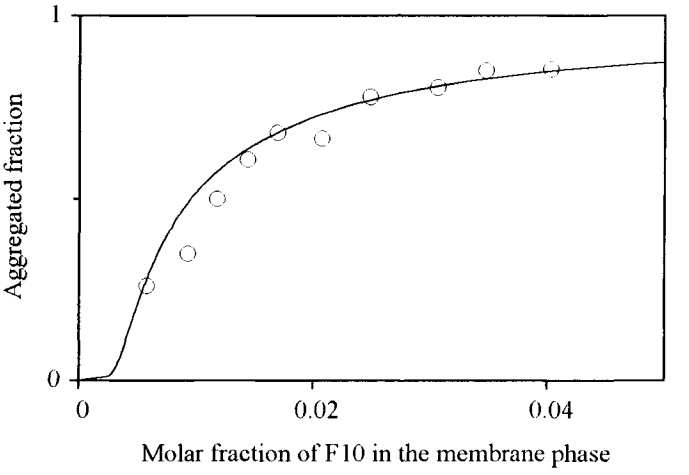

Figure 2.11. Aggregation data of F10 in membrane, as obtained by the results reported in Figure 2.9. The solid line is the best fit, according to Eq. (5).

To get further evidence of peptide aggregation inside the membrane, fluorescence resonance energy transfer (FRET) experiments were carried out by mixing together F10 and A3 in 2 mM lipid solution, the probes in the analogs being able to act as a FRET donor-acceptor pair. The Förster radius for the fluorene-azulene pair, calculated according to the following expression,[9,26,27] is $R_0 = 22$ Å.

$$R_0 = \left[\frac{2}{3} \alpha n^{-4} \Phi_D J \right]^{1/6} \quad (7)$$

In Eq. (7), n is the refractive index of the medium, Φ_D the quantum yield of the donor, α a constant ($8.785 \cdot 10^{-25}$ $M \cdot cm^{-1}$), and J the overlap integral of the normalized fluorescence spectrum of the donor and the absorption spectrum of the acceptor.

Owing to the strong distance dependence of FRET, the transfer efficiency is expected to vary significantly on going from a random distribution of fluorophores to the clustering caused by aggregation.[28,29] This is indeed the case, as shown in Figure 2.12, where the energy transfer efficiency as a function of acceptor (A3) concentration is reported together with that theoretically expected for a random distribution of peptide in the bilayer.[17] The quenching efficiency was assessed by the decrease in the average fluorescence lifetime of

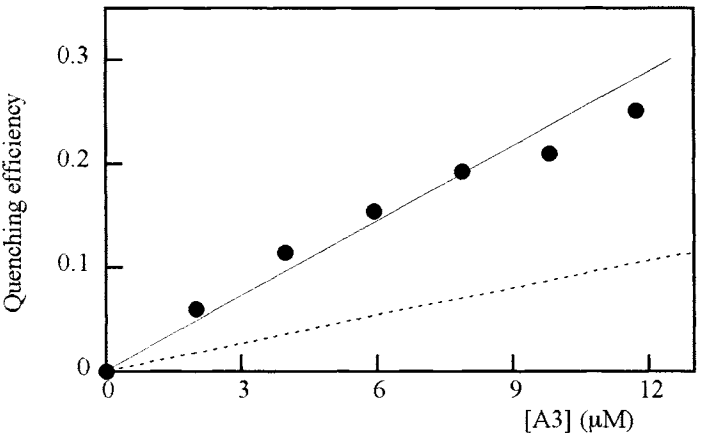

Figure 2.12. Efficiency of intermolecular fluorescence resonance energy transfer between F10 and A3 analogs in membrane, as a function of the acceptor concentration (full symbols). [Lipid] = 2 mM, [F10] = 2 μM, λ_{ex} = 265, λ_{em} = 315 nm. The quenching efficiency theoretically calculated for a random distribution of peptides in membrane is also reported, for comparison (broken line). The 2 mM membrane concentration corresponds approximately to a complete binding of the peptide.

the donor, to avoid inner-filter effects, caused by the acceptor absorption.[30] The large difference between the experimental and theoretical curves definitely indicate that gathering occurs in membrane, whose driving force can rely on different effects. It has been reported[31], for instance, that hydrophobic mismatch, i.e. the difference between the thickness of the hydrophobic core of the bilayer and the size of the transmembrane inclusion, may improve self-association. Moreover, specific intermolecular interactions are likely to arise from the GxxxG sequence motif, present in the primary structure of trichogin, where G stands for glycine and x for any aminoacid,[32] because the two glycine residues lie on the same face of the helical peptide, thus allowing a close, energetically favored intermolecular packing.

Finally, it is worth anticipating that a change in orientation of the peptide inside the membrane does take place, too, as the the membrane-bound peptide/lipid molar ratio (r) increases. The two phenomena are very likely concerted, in the sense that a transition to a transmembrane topology makes enough room for the peptide to aggregate.

2.5. BIOACTIVITY: MECHANISM OF MEMBRANE PERTURBATION

We next addressed the problem of the role played by the two membrane-bound species, M' and M'_n, in the bioactivity. The peptide-induced membrane permeability was then investigated, searching for a relationship between the variation in the concentration of M' or M'_n and peptide activity. Such relationship was indeed observed only when the membrane-bound M'_n species is taken into account, a finding suggestive that only the aggregate is responsible for membrane perturbation, and hence bioactivity. This is shown in Figure 2.13, where the membrane-bound aggregate, as determined by the relative population of the 2.2 ns lifetime component in the fluorescence decay, and bioactivity, expressed in terms of the initial rate of carboxyfluorescein release from the membrane, are reported as a function of F10 concentration. In the same Figure, the membrane-bound monomer concentration is also reported, whose trend emphasizes the close relationship existing solely between aggregate formation and membrane permeability.

To gather further informations on the mechanism of bioactivity, both light scattering and release experiments were carried out. Where the liposome content is released by disruption of the bilayer through a detergent-like mechanism, a drastic decrease in particle size, and hence in light scattering, is expected to occur.[31] This is indeed the case when a detergent, such as Triton, is added to the membrane, because a 15 times decrease in the intensity of light scattering is observed for liposome micellization. By contrast, upon addition of F10, A3 or TR-OMe at a concentration that causes an almost complete release of liposome content, the light scattering modestly varies (less than 10 %), implying that, in this case, the size of vesicles is not significantly perturbed. In addition, where the release of carboxyfluorescein and Texas-red labeled

dextran[@] is compared, the latter molecule is released in a much smaller quantity than the former one, at all peptide concentrations examined (data not shown).[17] Both these results rule out any mechanism of peptide-induced perturbation other than that involving peptide aggregates, which can be safely considered as the major contributor to the formation of transmembrane pores.

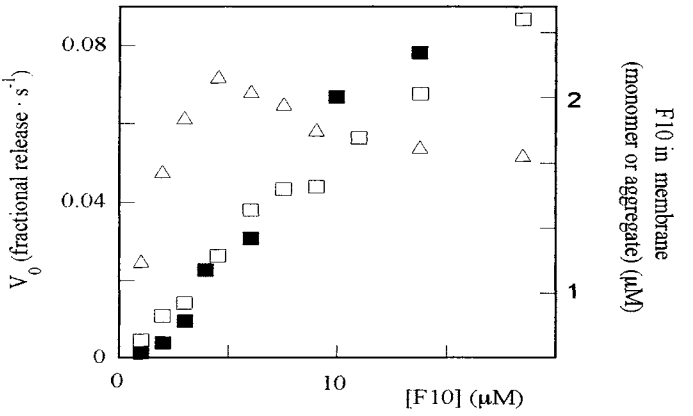

2.13. Relationship between the concentration of F10 aggregate in membrane (empty squares; right scale) and peptide activity (full squares; left scale), as a function of [F10]. Peptide activity is expressed in terms of the initial rate of carboxyfluorescein release from 0.2 mM ePC/cholesterol (1:1), after 20 min of peptide addition. The trend of the membrane-bound monomer concentration is also reported (triangles; right scale), showing the lack of any correlation with activity.

2.6. POSITION OF TRICHOGIN INTO THE MEMBRANE: TRANSLOCATION, DEPTH-DEPENDENT QUENCHING, AND DISTRIBUTION ANALYSIS

To tackle the problem of peptides translocation across the bilayer, FRET measurements, relying on the comparison of three different energy-transfer efficiencies rather than only two, as usually done,[33,34] were carried out. The position of trichogin analogs into the bilayer was also investigated by means of depth-dependent quenching experiments,[35] and distribution analysis of membrane quenching.[36,37]

2.6.1. Peptide Translocation

Liposomes containing the NBD energy-transfer acceptor,* and denoted as C6-NBD-PC(1-palmitoyl-2-[6-((7-nitrobenz-2-oxa-1,3-diazol-4- yl) amino)

[@] M.w. of carboxyfluorescein: 376; average m.w. of Texas-red labeled dextran: 10000.
* NBD = 7-nitrobenz-2-oxa-1,3-diazol-4-yl.

caproyl]-L-α-phospha-tidylcholine), were used for FRET experiments. Three samples were prepared, differing for the position of NBD in the bilayer, i.e. i) a symmetrically labeled liposome (s-L), where the fluorescent lipid is inserted in both layers by mixing it to the other components before membrane formation; ii) an outer layer labeled liposome (o-L), where the fluorescent probe is incorporated only in the external region of the membrane, as obtained by adding it to a bilayer suspension after liposome formation; iii) an inner layer labeled liposome (i-L), as obtained by chemically quenching the label in the outer layer of s-L liposomes.[38]

FRET depends on the inverse of the sixth power of the distance, the 50% quenching efficiency occurring at the interprobe distance R_0 (Förster radius).[9,26,27] In the case of F10, the fluorene-NBD pair has $R_0 = 24$ Å, while the thickness of the bilayer is 42 Å.[39] This ensures that a transbilayer FRET does not occur because of the small value of the Förster radius as compared to the thickness of the membrane. Since the fluorophore in C6-NBD-PC is located in the region of the polar headgroups,[40,41] quenching of the peptide lying in the outer layer or distributed in both leaflets of the bilayer is expected to be quite different. Upon translocation, one can predict that the quenching efficiency of i-L and o-L liposomes is approximately half that of the symmetrically labeled liposomes (s-L), where all peptides are surrounded by FRET acceptors. This because, on the average, half peptide molecules bound to i-L or o-L samples are in a layer void of acceptors. On the other hand, the relative increase in lipid fluorescence, as due to peptide binding, should be the same in all cases, because all labeled lipids are surrounded by peptide donors.

The aforementioned predictions were fully matched, as shown in Table 2.1, where the efficiency of relative fluorescence quenching of the donor [$E = 1 - (F/F_0)$], and the intensity increase of the acceptor (F'/F_0'), are reported. The relative fluorescence quenching of the donor was obtained normalizing the emission intensity F in the presence of acceptor labeled liposomes (s-L, o-L or i-L) by the fluorescence of the unlabeled sample (F_0). By contrast, the intensity increase in the acceptor emission caused by FRET was determined by measuring the lipid fluorescence in the presence (F') and absence (F_0') of the fluorescent peptide.

By inspection of the Table, it appears that i) the intensity increase of the acceptor is practically the same for all lipidic samples used. This because, once translocation occurs, in each layer the acceptor encounters, on the average, the same number of donors; ii) the quenching efficiency of the donor nearly doubles on going from o-L and i-L to s-L, as expected. These data clearly indicate the occurrence of a complete translocation of the peptide across the membrane. It is worth noting that, where translocation had not occurred, the i-L liposomes would have caused negligible quenching of peptide fluorescence, because all peptides would be lain in the outer layer, while the effect of o-L and s-L liposomes would have been the same, because both these membranes have the same amount of acceptors in the outer layer. As a result, the increase in lipid fluorescence would have been quite different from that observed.

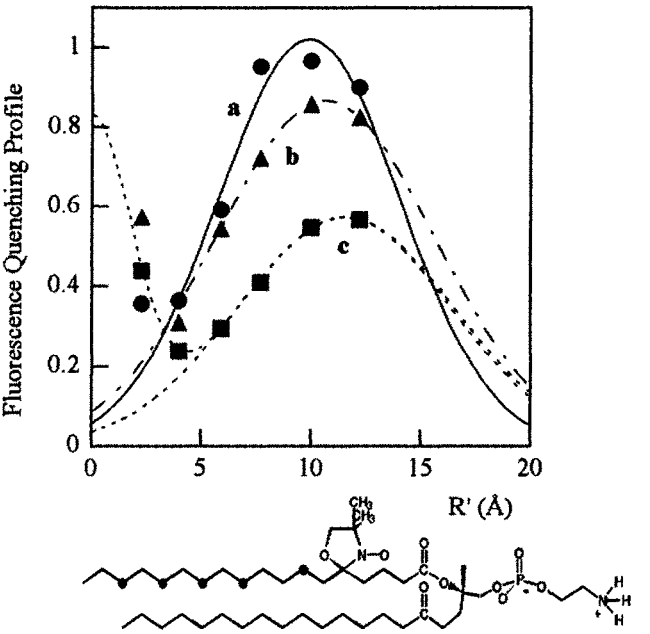

Figure 2.14. Fluorescence quenching profiles as a function of the distance from the bilayer center, R' (Å), generated by the distribution analysis of the membrane-inserted F10 peptide, at 0.5 μM (a), 3.5 μM (b) and 10.8 μM (c), in 2 mM labeled liposomes aqueous solution (λ_{ex} = 290, λ_{em} = 315 nm). The distribution appears doubly peaked, as explicitly shown by the fitting of curve c, because a single gaussian is unable to fit all experimental data (see text). In all cases, the second peak is much closer to the center of the bilayer. A schematic representation of a lipid molecule is reported at the bottom of the Figure, in which the possible quencher positions along the stearoyl chain are indicated by a full circle.

Table 2.1. Results of translocation experiments of F10 inside the three labeled liposomes, expressed as quenching efficiency for the fluorene donor (E) and intensity increase (F'/F_0') for the NBD acceptor. [a]

Liposomes	$E = 1 - (F/F_0)$ (donor)	F'/F_0' (acceptor)
o-L	0.19 ± 0.02	2.0 ± 0.2
i-L	0.23 ± 0.03	1.9 ± 0.2
s-L	0.34 ± 0.03	1.9 ± 0.2

a. All data were obtained using a peptide concentration of 0.5 μM.

2.6.2. Depth-Dependent Quenching and Peptide Distribution Analysis

A detailed information on the position of a fluorophore within a membrane can be obtained by the method of depth-dependent quenching,[35] based on exploiting quenchers covalently bound to the phospholipid acyl chains. By varying the quencher position along the lipid acyl chain, the depth of a fluorophore within a membrane can be explored. The experiments were carried out with F10 at three concentrations, i.e. 0.5, 3.5 and 10.8 μM, covering the whole activity range, corresponding to the release of membrane-entrapped carboxyfluorescein of 0%, 50% and 100%, respectively. The results are illustrated in Figure 2.14, where the profiles generated by the distribution analysis of the membrane-inserted peptide are reported as a function of the distance from the bilayer center, R' (Å). The inferences to be drawn from the data of this Figure are the following. i) In all cases, the distribution appears doubly peaked, because a single gaussian is inadequate to fit all experimental data. The second peak, explicitly shown only in the case of curve c, for the sake of clarity, is much closer to the center of the bilayer; ii) the ratio of the area under the peaks was estimated to be approximately 11 (curve a), 7 (b) and 4 (c), indicating that the amount of the peptide deeply buried into the membrane increases as F10 concentration increases; iii) at 0.5 μM, the highest decrease in fluorescence intensity is caused by the liposome having the quencher in position 7, which is near the polar headgroups; iv) at both 3.5 and 10.8 μM (curves b and c in Figure 2.14), i.e. at concentrations high enough to determine liposome leakage, the relative quenching efficiency that increases significantly is that corresponding to the liposome with the deepest quencher, according to the ratio of the area under the peaks, which is almost halved or quartered, respectively. These results once againg indicate that the peptide becomes depeely buried in the bilayer upon increasing the membrane-bound peptide/lipid molar ratio, r.

An independent confirmation of the foregoing results was obtained by performing similar experiments, but with different labeled lipids. As r rises, the fluorophore is becoming, on the average, more accessible to the quencher positioned close to the center of the bilayer. This is shown in Figure 2.15, where the ratio of fluorescence intensities, measured in the presence of liposomes containing stearic acids labeled in position 5 or 16 of the acyl chain, is reported. As may be seen, the F(16)/F(5) ratio decreases with a non-linear trend as the membrane-bound peptide/lipid molar ratio increases, because of the concomitant variation of the two intensities, the first increasing and the other one decreasing. The same effect is observed with A3, despite the fact that in this peptide the fluorescent label is close to the N-terminus rather than to the C-terminus, as in F10. This implies that the increase in the relative efficiency of the quencher located deeply in the bilayer is the same, irrespective of the direction taken by the peptide in going inside the membrane.

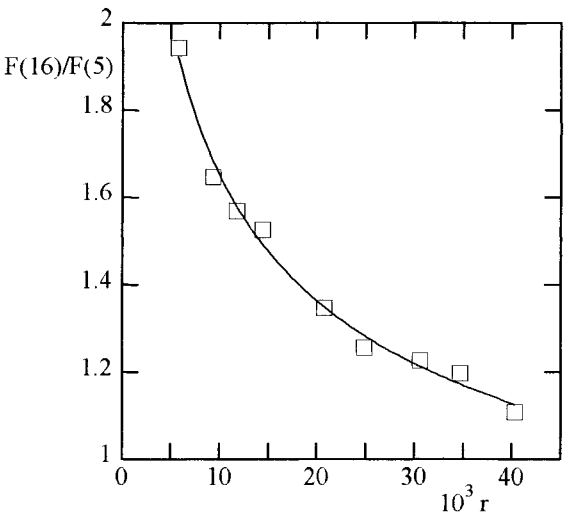

Figure 2.15. Relative quenching of F10 by liposomes containing stearic acid labeled on the 5th or 16th position by doxyl moiety, expressed as the ratio of fluorescence intensities of the peptide interacting with the two samples, as a function of the membrane-bound peptide/lipid molar ratio, r. [Lipid] = 2 mM; λ_{ex} = 265, λ_{em} = 315 nm.

2.7. PEPTIDES ORIENTATION INSIDE THE MEMBRANE

The results reported in Section 2.6.2 prove that trichogin changes its position in the lipid bilayer as the membrane-bound peptide/lipid molar ratio rises. At low r values, the peptides lie close to the polar headgroups region, but as r increases, reaching a value corresponding to a peptide concentration able to cause membrane leakage, the quenching efficiency of the doxyl group positioned approximately in the middle of the bilayer increases significantly. Therefore, under these conditions, the peptide in the membrane experiences both a gathering (Figure 2.12) and a diving-like process (Figure 2.15).

The change in orientation is thus strictly related to aggregation, as further illustrated in Figure 2.16, where both the fluorescence quenching data of F10 in lipids labeled with a quencher on the 5th or 16th position and the fraction of membrane-bound aggregate are plotted as a function of the membrane-bound peptide/lipid molar ratio. The {I(5)-I(16)}/[F10] quantity is, in fact, linearly related to the fraction of deeply buried peptide, representing the difference between the fluorescence intensities of F10 in the lipids labeled with a quencher on the 5th or 16th position, as obtained from the data of Figure 2.15, normalized by the peptide concentration in the membrane. A similar trend was observed for A3 analog, too. From the results, it appears that there is a strict relationship between the two sets of data, suggesting that F10, and hence trichogin, populates two states only, i.e. a monomeric, surface bound and inactive form, and a buried, aggregated state, responsible for membrane leakage. There is,

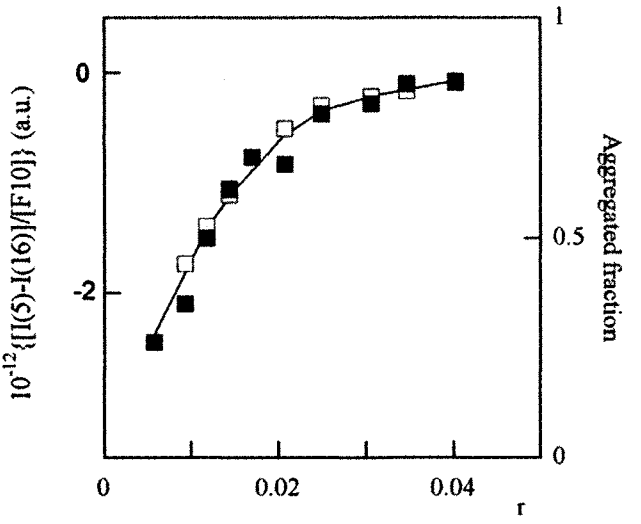

Figure 2.16. Dependence of the fraction of membrane-bound F10 aggregate (full symbols) and of the same peptide deeply buried into the bilayer (empty symbols) on the membrane-bound peptide/lipid molar ratio, r. The {I(5)-I(16)}/[F10] quantity is linearly related to the fraction of deeply buried peptide, [F10] representing the peptide concentration in the membrane (see text).

therefore, a threshold for the transition to a transmembrane orientation, and the interconversion between the two states is controlled by the membrane-bound peptide/lipid molar ratio.

A concentration-induced orientational transition, like that above described, was already reported for a few other antibiotic peptides,[42] as well as for the antifungal polyene nystatin.[43] This phenomenon can be explained by considering that a perturbation of the surface tension of the membrane arises from the binding of the peptide to the surface,[6] and that at high peptide concentration excluded volume effects come also into play.[44] As a result, at fixed lipid concentration, a transmembrane orientation becomes thermodinamically favored as the amount of peptide increases.

The features of the transmembrane arrangement depend on the charge state of the peptide. For neutral or weakly charged peptides, such as alamethicin, a full insertion into the lipid bilayer is feasible, while for highly charged peptides, such as magainin, the insertion in the apolar region of the membrane is unfavored. In the latter case, an increase in peptide concentration leads to the formation of bilayer defects, the so-called "toroidal pores", which is another way in which a relaxation process for the accumulated surface tension is thought to occur.[2] Accordingly, the foregoing results indicate that a high value of r forces the neutral lipopeptide trichogin to go deeply inside the bilayer.

An earlier study[45] - in which both a trichogin analog containing the quencher aminoacid TOAC and liposomes labeled with phosphatidylcholine analogs, bearing the fluorophore BODIPY* at different positions along the acyl chain, were used - apparently contradicts this conclusion. Because the fluorescence quenching was found to be independent of the position of TOAC in the peptide and of the peptide/lipid ratio, the idea was that trichogin was lying along the membrane surface, at all concentrations examined. However, it has been conclusively shown[46] that the BODIPY group attached to phospholipids exhibits a clear tendency to reside in the polar headgroups region of the bilayer, irrespective of its position along the acyl chain. Therefore, we are highly inclined to think that, using this fluorophore, in no case a transition in peptide orientation could be detected. This idea is supported by the lack of any clear dependence of fluorescence quenching on BODIPY position along the lipid acyl chain (Figure 2.2 of ref. 45), indicating that the fluorescent lipid analog employed makes it impossible to determine the actual peptide position inside the membrane. By contrast, the data presented here have not such limitation,[47] because the use of doxyl labeled lipids and fatty acids is a very well established method for determining the membrane position of fluorescent probes.[33,35] It must be also mentioned that some EPR results[48] support the hypothesis put forward in ref. 45. However, the 0.1 mM peptide concentration used in this study is definitely higher than that normally needed for antimicrobial and membrane perturbing activity, and too high to make the EPR data and those reported here worthy of comparison, also in view of the complex interplay between the strongly concentration-dependent aggregation and membrane-peptide partition phenomena.[47]

2.8. CONCLUDING REMARKS

From the data set considered here, four major conclusions can be drawn. Firstly, the analogs of trichogin GA IV investigated exhibit structural features and bioactivity very similar to that of the natural peptide, and undergo a monomer-aggregate equilibrium both in water and model membranes. The aggregates in the two phases differ, however, in size and, possibly, structure. Secondly, fluorescence quenching measurements, carried out using water soluble quenchers and quenchers positioned in the membrane at different depths, indicate that at low membrane-bound peptide/lipid molar ratio (r) trichogin lies close to the region of polar headgroups, while, as r increases until membrane leakage occurs, a cooperative transition takes place, leading to an arrangement that sees the peptide deeply buried into the bilayer. Thirdly, the transitions from a surface to a transmembrane topology and from monomers to oligomers are very likely concerted, in the sense that a transmemrane arrangement makes enough room for the peptide to aggregate. Fourthly, Förster

* TOAC = 4-amino-4 carboxy-2,2,6,6-tetramethylpiperidino-1-oxyl; BODIPY = 4,4-difluoro-4-bora-3a,4a- diaza-S-indacene).

energy transfer measurements indicate that, on the average, trichogin is equally distributed between the outer and inner leaflet of the membrane.

The mechanism of trichogin action can be then envisaged as a two-state transition controlled by peptide concentration. One state is the monomeric, surface bound and inactive peptide, and the other state is a buried, aggregated form, which is responsible for membrane leakage and bioactivity. Since trichogin suffers of hydrophobic mismatch, a complex supramolecular structure is likely to form when the peptide is buried into the bilayer, [49] an hypothesis which is under investigation.

2.9. ACKNOWLEDGMENTS

We thank Prof. C. Toniolo for kindly providing the trichogin analogs, and the Ministry of University and Research for financial support.

2.10. REFERENCES

1. N. Sewald, and H.-D. Jakubke, *Peptides:Chemistry and Biology* (Wiley-Vch, Weinheim, 2002).
2. Y. Shai, Mode of action of membrane active antimicrobial peptides, *Biopolymers* **66**, 236-248 (2002).
3. R. M. Epand, and H. J. Vogel, Diversity of antimicrobial peptides and their mechanisms of action, *Biochim. Biophys. Acta* **1462**, 11-28 (1999).
4. K. Matsuzaki, Molecular mechanisms of membrane perturbation by antimicrobial peptides, in *Development of Novel Antimicrobial Agents*: *Emerging Strategies*, edited by K. Lohner (Horizon Scientific Press, Wymondham, 2002), pp.167-181.
5. L. Yang, T. A. Harroun, T. M. Weiss, L. Ding, and H. W. Huang, Barrel stave or toroidal model? A case study on melittin pores, *Biophys. J.* **81**, 1475-1485 (2001).
6. F. Y. Chen., M. T. Lee, and H. W. Huang, Sigmoidal concentration dependence of antimicrobial peptide activities: a case study on alamethicin, *Biophys. J.* **82**, 908-914 (2002).
7. C. Toniolo, M. Crisma, F. Formaggio, C. Peggion, R. F. Epand, and R. M. Epand, Lipopeptaibols, a novel family of membrane active, antimicrobial peptides, *Cell. Mol. Life Sci.* **58**, 1179-1188 (2001).
8. B. Pispisa, L. Stella, M. Venanzi, A. Palleschi, F. Marchiori, A. Polese, A., and C. Toniolo, A spectroscopic and molecular mechanics investigation on a series of Aib-based linear peptides and a peptide template, both containing tryptophan and a nitroxide derivatives as probes, *Biopolymers* **53**, 169-181 (2000).
9. B. Pispisa, L. Stella, M. Venanzi, A. Palleschi, C. Viappiani, A. Polese, F. Formaggio, and C. Toniolo, Quenching mechanisms in bichromophoric, 3_{10}-helical Aib-based peptides, modulated by chain-length dependent topologies, *Macromolecules* **33**, 906-915 (2000).
10. P. Scrimin, P. Tecilla, U. Tonellato, A. Veronese, M. Crisma, F. Formaggio, and C. Toniolo, Zinc(II) as an allosteric regulator of liposomal membrane permeability induced by synthetic template-assembled tripodal polypeptides., *Chem. Eur. J.* **8**, 2753-2763 (2002).
11. A. D. Milov, Y. D. Tsvetkov, F. Formaggio, M. Crisma, C. Toniolo, and J. Raap, Self-assembling and membrane modifying properties of a lipopeptaibol studied by CW-ESR and PELDOR spectroscopies, *J. Pept. Sci.* **9**, 690-700 (2003).
12. B. Pispisa, A. Palleschi, C. Mazzuca, L. Stella, A. Valeri, M. Venanzi, F. Formaggio, C. Toniolo, and Q. B. Broxterman, The versatility of combining FRET measurements and molecular mechanics results for determining the structural features of ordered peptides in solution, *J. Fluoresc.* **12**, 213-217 (2002).
13. C. Toniolo, A. Polese, F. Formaggio, M. Crisma, and J. Kamphuis, Circular dichroism spectrum of a peptide 3_{10}-helix, *J. Am. Chem. Soc.* **118**, 2744-2745 (1996).

14. B. Pispisa, C. Mazzuca, A. Palleschi, L. Stella, M. Venanzi, F. Formaggio, C. Toniolo, and Q. B. Broxterman, Structural features and conformational equilibria of 3_{10}-helical peptides in solution by spectroscopic and molecular mechanics studies, *Biopolymers (Biospectroscopy)* **67**, 247-250 (2002).
15. W. C. Wimley, and S. H. White, Experimentally determined hydrophobicity scale for proteins at membrane interfaces, *Nat. Struct. Biol* **3**, 842-848 (1996).
16. S. H. White, and W. C. Wimley, Hydrophobic interactions of peptides with membrane interfaces, *Biochim. Biophys. Acta* **1376**, 339-352 (1998).
17. L. Stella, C. Mazzuca, M. Venanzi, A. Palleschi, M. Didonè, F. Formaggio, C. Toniolo, and B. Pispisa, Aggregation and water-membrane partition as major determinants of the activity of the antibiotic peptide trichogin GA IV, *Biophys. J.* **86**, 936-945 (2004).
18. V. Rizzo, S. Stankowski, and G. Schwarz, Alamethicin incorporation in lipid bilayers: a thermodynamic study, *Biochemistry* **26**, 2751-2759 (1987).
19. M. Castanho, and M. Prieto, Filipin fluorescence quenching by spin-labeled probes: studies in acqueous solution and in a membrane model system, *Biophys. J.* **69**, 155-168 (1995).
20. A. S. Ladokhin, and S. H. White, Alphas and taus of tryptophan fluorescence in membranes, *Biophys. J.* **81**, 1825-1827 (2001).
21. H. W. Huang, Action of antimicrobial peptides: two-state model, *Biochemistry* **39**, 8347-8352 (2000).
22. S. H. White, and W. C. Wimley, Membrane protein folding and stability: physical principles, *Annu Rev. Biophys. Biomol. Struct.* **28**, 319-365 (1999).
23. T. J. McIntosh, A. Vidal, and S. A. Simon, The energetics of peptide-lipid interactions: modulation by interfacial dipoles and Cholesterol, in *Peptide-Lipid Interactions*, edited by T. J. McIntosh, and S. A. Simon (Academic Press, San Diego 2002), pp. 309-338.
24. C. J. Russell, T. E. Thogeirsson, and Y. –K. Shin, The membrane affinities of the aliphatic amino acid side chains in an alpha-helical context are independent of membrane immersion depth, *Biochemistry* **38**, 337-346 (1999).
25. C. Tanford, *The Hydrophobic Effect: Formation of Micelles and Biological Membranes*, 2nd ed. (Wiley, New York, 1980).
26. B. Pispisa, M. Venanzi, L. Stella, A. Palleschi, A., and G. Zanotti, Photophysical and structural features of covalently bound peptide-protoporphyrin-peptide compounds carrying naphtalene chromophores, *J. Phys. Chem. B* **38**, 8172-8179 (1999).
27. L. Stella, M. Venanzi, M. Carafa, E. Maccaroni, M. E. Straccamore, G. Zanotti, A. Palleschi, and B. Pispisa, Structural features of model glycopeptides in solution and in membrane phase: a spectroscopic and molecular mechanics investigation, *Biopolymers* **64**, 44-56 (2002)
28. M. Schümann, M., Dathe, M., Wieprecht, T., Beyermann, M., and M. Bienert, The tendency of magainin to associate upon binding to phospholipid bilayers, *Biochemistry* **36**, 4345-4351 (1997).
29. J. Strahilevitz, A. Mor, P. Nicolas, and Y. Shai, Spectrum of antimicrobial activity and assembly of dermaseptin-b and its precursor form in phospholipid membranes, *Biochemistry* **33**, 10951-10960 (1994).
30. B. Pispisa, C. Mazzuca, A. Palleschi, L. Stella, M. Venanzi, M. Wakselman, J. –P. Mazaleyrat, M. Rainaldi, F. Formaggio, and C. Toniolo, A combined spectroscopic and theoretical study of a series of conformationally restricted hexapeptides carrying a rigid binaphthyl-nitroxide donor-acceptor pair, *Chem. Eur. J.* **9**, 2-11 (2003).
31. G. R. Jones, and A. R. Cossins, Physical methods of study, in *Liposomes: a Practical Approach*, edited by R. R. C. New (Oxford University Press, Oxford., 1990) pp. 183-220.
32. A. R. Curran, and D. M. Engelman, Sequence motifs, polar interactions and conformational changes in helical membrane proteins, *Curr Op. Struct. Biol.* **13**, 412-417 (2003).
33. K. Matsuzaki, O. Murase, N. Fujii, and K. Miyajima, Translocation of a channel forming antimicrobial peptide, magainin 2, across lipid bilayers by forming a pore, *Biochemistry* **34**, 6521-6526 (1995).
34. W. C. Wimley, and S. H. White, Determining the membrane topology of peptides by fluorescence quenching. *Biochemistry* **39**, 161-170 (2000).
35. E. London, and A. S. Ladokhin, Measuring the depth of amino acid residues in membrane-inserted peptides by fluorescence quenching, in *Peptide-Lipid Interactions*, edited by T.J. McIntosh, and S.A Simon (Academic Press, San Diego 2002) pp. 89-115.

36. A. S. Ladokhin, Distribution analysis of depth-dependent fluorescence quenching in membranes: a practical guide, *Meth. Enzymol.* **278**, 462-473 (1997).
37. A. S. Ladokhin, Analysis of protein and peptide penetration into membranes by depth-dependent fluorescence quenching: theoretical considerations, *Biophys. J.* **76**, 946-955 (1999).
38. J.C. McIntyre, and R.G. Sleight, Fluorescence assay for phospholipid membrane asimmetry, *Biochemistry* **30**, 11819-11827 (1991).
39. L. J. Lis, M. McAlister, N. L. Fuller, R. P. Rand, and V. A. Parsegian, Measurement of the lateral compressibility of several phospholipid bilayers, *Biophys. J.* **37**, 667-672 (1982).
40. S. Mazeres, V. Schram, J. F. Tocanne, and A. Lopez, 7-Nitrobenz-2-oxa-1,3-diazole-4-yl-labeled phospholipids in lipid membranes: differences in fluorescence behavior, *Biophys. J.* **71**, 327-335 (1996).
41. D. E. Wolf, A. P. Winiski, A. E. Ting, K. M. Bocian, and R. E. Pagano, Determination of the transbilayer distribution of fluorescent lipid analogues by nonradiative fluorescence resonance energy transfer, *Biochemistry* **31**, 2865-2873 (1992).
42. M. Lee, F. Chen, and H. W. Huang, Energetics of pore formation induced by membrane active peptides, *Biochemistry* **43**, 3590-3599 (2004).
43. A. Coutinho, and M. Prieto, Cooperative partition model of nystatin interaction with phospholipid vesicles, *Biophys. J.* **84**, 3061-3078 (2003).
44. M. Zuckermann, and T. Heimburg, Insertion and pore formation driven by adsorption of proteins onto lipid bilayer membrane-water interfaces, *Biophys. J.* **81**, 2458-2472 (2001).
45. R. F. Epand, R. M. Epand, V. Monaco, S. Stoia, F. Formaggio, M. Crisma, and C. Toniolo, The antimicrobial peptide trichogin and its interaction with phospholipid membranes, *Eur. J. Biochem.* **266**, 1021-1028 (1999).
46. R. D. Kaiser, and E. London, Determination of the depth of BODIPY probes in model membranes by parallax analysis of fluorescence quenching, *Biochim. Biophys. Acta* **1375**, 13-22 (1998).
47. C. Mazzuca, L. Stella, M. Venanzi, F. Formaggio, C. Toniolo, and B. Pispisa, Mechanism of membrane activity of the antibiotic trichogin GA IV: a two-state transition controlled by peptide concentration, *Biophys. J.* **88**, 3411-3421 (2005).
48. V. Monaco, F. Formaggio, M. Crisma, C. Toniolo, P. Hanson, and G. L. Millhauser, Orientation and immersion depth of a helical lipopeptaibol in membranes using TOAC as an ESR probe, *Biopolymers* **50**, 239-253 (1999).
49. M. R. R. de Planque, and J. A. Killian, Protein-lipid interactions studied with designed transmembrane peptides: role of hydrophobic matching and interfacial anchoring, *Mol. Membr. Biol.* **20**, 271-284 (2003).